Impurities in a High Temperature PEM Fuel Cell: Focus on Unconverted Methanol

Samuel Simon Araya

Pontoppidanstræde 101
Aalborg East 9220
Denmark
E-mail: ssa@et.aau.dk

Søren Juhl Andreasen , Søren Knudsen Kær

Abstract

In this work the effects of reformate gas impurities on a H_3PO_4-doped polybenzimodazole (PBI) membrane-based high temperature proton exchange membrane fuel cell (HT-PEMFC) are studied. A unit cell assembly with a BASF Celtec®-P2100 high temperature membrane electrode assembly (MEA) of active surface area of 45 cm^2 is investigated by means of impedance spectroscopy. The concentrations in anode feed gas of all impurities, unconverted methanol-water vapor mixture, CO and CO_2 were varied along with current density according to a multilevel factorial design of experiments. Results showed that all the impurities degrade the performance with CO being the most degrading agent and CO_2 the least. A statistical analysis showed that there is interdependence among the effects of the different factors considered. This interdependence suggests that tolerances to concentrations of CO, above 2% may be compromised by the presence in the anode feed of CO_2. Methanol showed a poisoning effect on the cell at all the tested feed ratios. The performance drop is found to be proportional to the amount of methanol in feed gas, and severe effects were seen when other impurities are also present, especially at higher methanol content in anode feed gas.

Keywords: HT-PEM, Fuel Cell, Methanol, CO_2, CO, Impedance Spectroscopy

1. Introduction

For fuel cell applications, methanol allows a more practical energy storage compared to either compressed or liquid hydrogen. It is liquid at room temperature, which makes its storage and distribution much less complicated than the required hydrogen infrastructure, as it can use existing gasoline infrastructure with only few modifications. Unlike natural gas, gasoline and other fossil fuel sources of hydrogen, it can be CO_2 neutral if prepared from renewables of various biomass sources such as wood, forest waste, peat, municipal solid wastes, sewage and even chemical recycling of CO_2 in the atmosphere [1, 2].

Moreover, owing to its lower-energy chemical bonds, i.e. the absence of C-C bonds, methanol has the advantage of requiring lower reforming temperatures of about 250 to 300 °C with respect to other hydrocarbon fuels, where the required temperature is 800 to 900 °C [3]. Methanol reforming temperature can further be reduced to around 200 °C, comparable to the operating temperatures of a HT-PEMFC, with good conversion efficiencies and low CO contents, but lower hydrogen yield [4]. This is desirable as it opens new opportunities, making methanol increasingly proposed for on-board reforming to hydrogen and carbon dioxide for indirect methanol fuel cells including HT-PEMFC [4, 5, 6].

In spite of the compelling advantages methanol has over other sources of hydrogen for use in fuel cells, the outcome of its steam reforming process is not hydrogen alone. It is a hydrogen rich mixture of gases and vapors, known as reformate gas, that contains a number of impurities that have potential poisoning effects on a fuel cell. These impurities are CO, CO_2 and unconverted methanol and water vapor mixture. Current steam methanol reforming technology gives reformate gas composed roughly of; 71% H_2, 25% CO_2, 1% CO and 3% unconverted methanol-water vapor mixture.

Recently, research has been focusing on characterizing the poisoning effects of CO and CO_2 in both low and high temperature PEM fuel cells, in order to understand the mechanisms by which they affect the performance of fuel cells [7, 8, 9, 10, 11]. It is widely recognized that CO is the main poison for the catalyst amongst the impurities in a reformate gas. It adsorbs at the surface of Platinum electro-catalyst and takes active sites that should otherwise be used for catalysis [9]. Tolerance of PEM fuel cells to the poisoning effect of CO increases with increase in temperature, one among several advantages of HT-PEMFC (operating optimally between 160 to 180 °C) over

low temperature PEM fuel cells (operating below 100 °C, typically around 80 °C). This is because increase in temperature favors H_2 adsorption over CO adsorption on Pt, due to the less exothermic nature of H_2 [9]. Moreover, increase in temperature promotes the electrooxidation of the adsorbed CO into CO_2 [12, 13], which only has a diluting effect and does not take up electro-active catalyst sites.

However, despite all the research recently done on the poisoning effects of CO and CO_2, studies on the possible poisoning effects of methanol vapor on HT-PEMFC is extremely scarce. The only knowledge about the effect of methanol on a PEM membrane comes from studies on direct methanol fuel cells (DMFC), where crossover through the membrane with subsequent oxidation on the cathode side is the main mechanism by which performance is degraded [14]. Such an effect may be expected on PBI based HT-PEMFCs as well, but this needs to be investigated through experiments.

The present work addresses these issues and includes the effects of unconverted methanol-water vapor mixture to the array of impurities to make the study of HT-PEMFC characterization more comprehensive. Electrochemical impedance spectroscopy (EIS) was chosen as a characterization technique, where several impedance measurements were taken at different operating conditions and varying feed gas compositions.

2. Methodology

In the following the experimental setup, a brief summary of impedance spectroscopy applied to fuel cells, and the experimental procedures are described.

2.1. Experimental Set-up

In Fig. 1 the complete setup used to characterize the effects of reformate gas impurities in an HT-PEMFC is illustrated. It consists of a unit HT-PEM fuel cell assembly, mass flow controllers and a vapor delivery system. A typical H_3PO_4-doped PBI-based MEA for HT-PEMFC, BASF Celtec®-P2100 MEA, with an active surface area of 45 cm^2 was employed.

The mass flow controllers allowed the entry into the fuel cell of the gaseous species involved, H_2 gas, CO_2, and CO on the anode side and air on the cathode side. A vapor delivery system was designed for the remaining constituents of the reformate gas, unconverted methanol vapor along with water

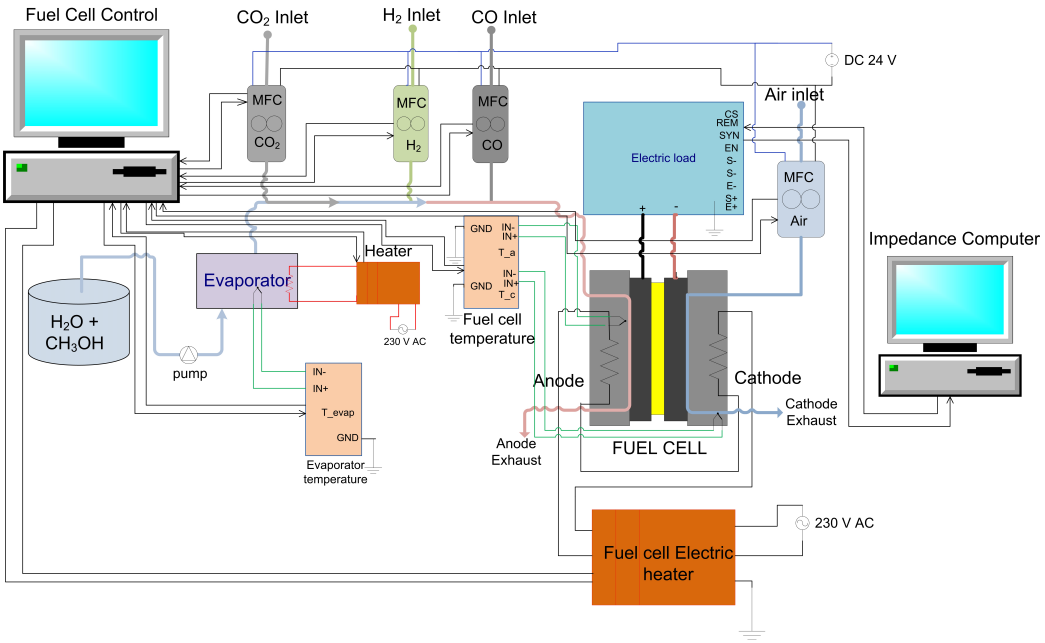

Figure 1: Experimental setup

vapor. This sytem, composed of a small high precision dosing pump (Watrson Marlow 120U) and an electrically heated evaporator, delivers the vapor mixture in a controlled manner and at a fixed steam to carbon ratio. It is described in detail in our previous work [15].

The setup is entirely controlled and monitored by a control program in a LabView® environment and impedance measurements were done with a separate Gamry FC350 hardware and control software. Apart from the vapor delivery sytem, the setup is identical to the one described in [7] .

2.2. Impedance Spectroscopy

Impedance spectroscopy, also know as electrochemical impedance spectroscopy (EIS) or AC impedance, is a technique of characterization of electrochemical devices. It is done by measuring the electrical response of a material to small induced signal perturbances. These are then analysed to obtain useful information about the behavior of the device under various conditions.

Impedance is a complex function that can be calculated by Eqn. (1), using the amplitudes of the current, the voltage and the phase shift.

$$Z = \frac{V_0\, e^{j(\omega t - \phi)}}{I_0\, e^{j\omega t}} = \frac{V_0}{I_0}\, e^{-j\phi} = Z_0\,(\cos\phi - j\sin\phi) \qquad (1)$$

In Eqn. (1), Z [Ω] is the complex impedance response of the system, V_0 [V] and I_0 [A] are the voltage and current signal amplitudes respectively, ω [rad s^{-1}] is the signal frequency and ϕ [rad] is the voltage phase shift. It has a real part ($Z_0 \cos\phi$) and imaginary part ($Z_0 j \sin\phi$), and is normally represented on a Nyquist curve with real part on the horizontal axis and the imaginary on the vertical axis.

In fuel cells, EIS was recently used extensively for optimization, characterization and diagnostics [16, 17, 18, 19, 20, 21]. The different processes that occur in a cell respond differently to perturbances over a broad range of frequencies. In fact, if a fuel cell is perturbed on a broad range of frequencies, at low frequency the effects on slower processes with longer time constant like diffusion will be registered. At higher frequency however, effects on charge transfer would be sensed as they are much faster and have a much shorter time constant. The technique is described in detail in [22, 23] for general application and in [16] for PEM fuel cells in particular.

One of the main advantages of EIS is that it is not intrusive and can be performed in-situ. It is a detailed technique with which information about different processes in the electrochemical device can be obtained with only little perturbation. Since the perturbances are very small compared to the measured DC voltage or current, changes within the cell are minimal [24]. In a PEM fuel cell an AC perturbance of $\sim$5 % of the measured DC value can be suitably used [25].

In order to translate impedance measurement in to more comprehensible figures and extract meaningful quantitative information, the analysis of data is typically done by fitting the measured data to an equivalent circuit model (EC) or a model based on physical properties, that can reasonably represent the fuel cell under investigation. For insight in the correct use of equivalent circuit modeling the reader is refered to [22, 23, 16].

2.3. Experimental Procedure

The fuel cell was allowed to break-in, at 0.2 A/cm^2 (9A), 160 °C for 100 hours. During break-in stoichiometric ratios of hydrogen, λ_{H_2} and air, λ_{Air} were kept constant at 2.5 and 3.5, respectively.

A full multilevel factorial design of experiments was chosen for thorough investigation of the effects of the different factors and their interdependence.

Table 1: The different factors and their levels used for the factorial design of experiments

Factor	levels		
Current Density [A/cm^2]	0.22	0.33	0.44
CO [% by volume]	0	1	2
CO_2 [% by volume]	0	20	
Methanol-Water vapor mixture [% by volume]	0	5	10

Four factors, namely current density, concentration of methanol-water vapor mixture, CO concentration and CO_2 concentration were varied. The different factors and how they were varied in increasing levels is summarized in tab. 1. A total of 54 runs are required for 3 levels of current density, methanol and CO concentrations, and 2 levels of CO_2. However, the most severe combinations that caused excessive voltage drop and system instability were excluded and therefore 38 of the required runs, with three replicates each were performed. Out of the replicates the best ones, i.e. the ones with the least noise were chosen for analysis.

The conditions that caused poor cell performance were the ones at current density of 0.44 A/cm^2 (20 A), where not all the impurities could be tested, especially in the presence of CO in the anode feed. Similar situation was observed at 0.33 A/cm^2 (15 A), when all the impurities were set to their highest levels and therefore, measurements in this case were limited to 1% CO and 5% methanol-water vapor mixture. Instability of the steady state equilibrium is also observed in [26] at high CO concentrations.

Temperature was kept constant at 160 °C throughout the duration of the experiments. The runs were not randomized in order to avoid too much disruption of the equilibrium state of the operating fuel cell which would lead to longer waiting time between successive runs and also perhaps to premature failure of the device under investigation. Therefore, according to experience, factors that affect the equilibrium state the least were allowed to vary the most and the degree of contamination was made to increase progressively in time. This way a maximum number of allowable runs was achieved. In appendix A the complete multilevel factorial design of the experiment with

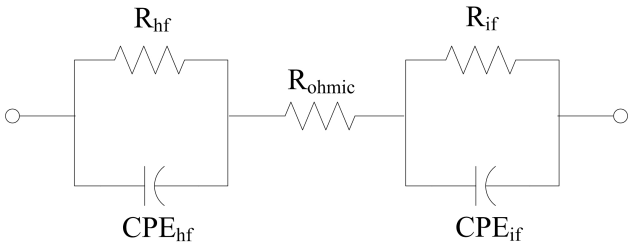

Figure 2: Equivalent circuit with constant phase elements (CPE) used in this work

fitted resistance responses is shown.

For the steam methanol reforming a steam to carbon ratio (S/C) of 1.5 was considered, which corresponds to 40% by volume of water and 60% by volume of methanol. It was assumed that the unconverted methanol-water vapor mixture would maintain the same S/C ratio of 1.5.

In this work a galvanostatic EIS is used, in which a perturbing AC current sinusoidal is applied and voltage response is registered. For this an AC sinusoidal of 0.5 A was applied, which is equals to 5% of the lowest current value (10 A) tested. This allows linearity assumption to hold for all measurements. Impedance spectra were acquired at different fuel cell operating conditions, while H_2 gas and air stoichiometric ratios were kept constant at 1.5 and 4, respectively. Measurements were done in the frequency range between 10 kHz and 1 Hz, and 10 points per decade were recorded.

For analysis and interpretation of impedance data, an EC model shown in Fig. 2 was chosen. It is composed of lumped resistance (R) in series with two circuits, each comprising a resistance and a constant phase element (CPE), parallel to each other. One of the resistances, R_{ohmic}, corresponds to the ohmic losses of the cell, which are mainly due to the electrolyte resistance and contact resistances between interfaces. The other two resistances, R_{hf} and R_{if}, are charge transfer resistances between electrode and electrolyte interfaces for high frequency range (10 kHz to $\sim$125 Hz) and intermediate-low frequency range ($\sim$125 Hz to 1 Hz), respectively, and are sometimes controversially split between anode and cathode contributions [27].

Constant phase elements are used instead of double layer capacitances to achieve better fits and their exponential coefficients, α were kept constant at 0.75 for all the fits. Only resistances are allowed to change in the fitting software, ZView^{TM} (Scribner Associates, Inc.). The software employs complex non linear least-square (CNLS) method for fitting and error estimation. For

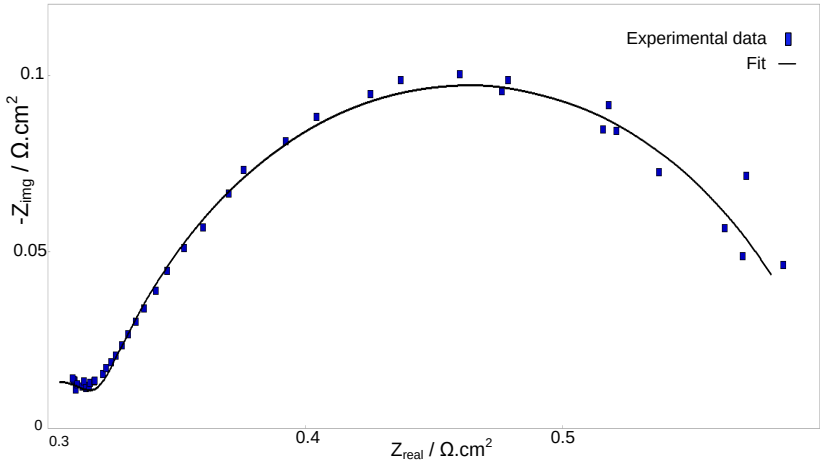

Figure 3: fitting between measured impedance data and the chosen equivalent circuit model

a better understanding of CNLS one can refer to [28]. The quality of the fit between the measured impedance data and the equivalent circuit model of choice is shown in Fig. 3.

3. Results

Results are divided into two subsections, where in the first a general statistical analysis on the mean values of the fitted data was performed and interdependence among factors was investigated. Then analysis was made on fitted resistance values according to the progression in which tests were conducted. To assist the analysis histograms were used to illustrate the trends of resistances for the different frequency ranges.

3.1. Statistical Analysis of Factors Interdependency

Statistical analyses were performed using Minitab®, statistical software. First the main effects of the various factors were analysed based on mean values of the fitted values of the resistances, then interactions among factors were assessed. Figure 4 illustrates the main effects of methanol, CO, CO_2 and current density for the different regions of the frequency sweep.

During the experiments, while there was almost no voltage drop observed before the introduction of the impurities, tests with impurities resulted in an overall average voltage drop rate of 0.76 mV/hr. This needs to be considered

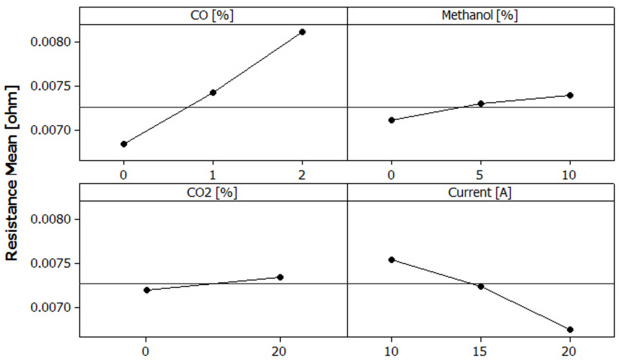

(a)

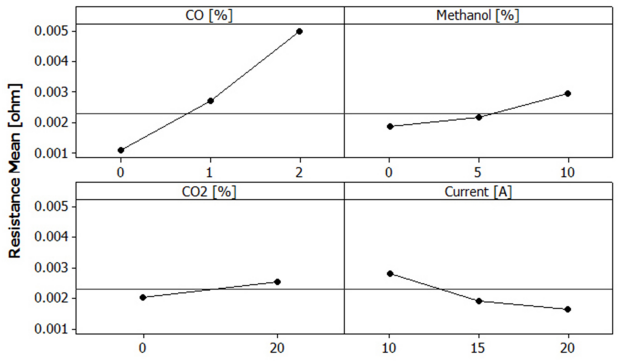

(b)

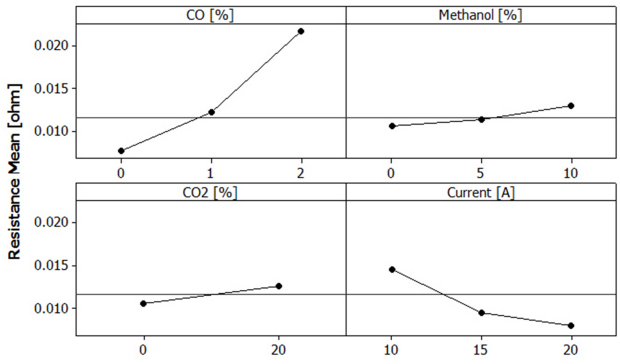

(c)

Figure 4: Main effects of each factor at 160 °C, (a) ohmic resistance (b) high frequency resistance (c) intermediate - low frequency resistance

as it is not known whether time affects the effects of the other factors and/or their interdependency. This could be investigated by including time as one of the factors and assessing its interaction with the rest of the factors. However, this is beyond the scope the present work and consequently experiments were not designed to include it.

It can be noticed that CO has the most poisoning effects of all in the whole frequency range while CO_2 has the least effects of all. Increase in current density causes decrease in resistance, and with the exception of the ohmic resistance the effect is more pronounced in going from 0.22 A/cm^2 to 0.33 A/cm^2 than from 0.33 A/cm^2 to 0.44 A/cm^2.

Increase in methanol concentration of the anode feed causes resistances to increase as in the case of CO and CO_2, with minimal increase, comparable to that of CO_2 observed for R_{ohmic} and R_{if}. The increase in is a little more pronounced for R_{hf}, especially when the concentration of methanol-water vapor mixture in anode feed gas is raised to 10% by volume.

Figure 5 shows the interactions among factors. In interaction plots, parallels lines show the absence of interaction between factors, while deviation from parallelism shows interaction of some sort. In Fig. 5(a) there seems to be very small or no interaction between the effects of CO and the other factors for R_{ohmic}. In the same plots it can be seen that increase in CO_2 content of the anode feed gas causes an increase in R_{ohmic} in the presence of 5% by volume of methanol vapor in feed gas. This interaction however disappears when the methanol concentration is raised to 10% by volume. As it can be seen in Fig. 5(b) and (c), this type of interaction persists throughout the whole range of frequencies.

The effect of methanol does not seem to depend on the rest of the impurities, as the quasi parallel lines of effects show in Fig. 5, except for a small interaction with CO_2 as mentioned above. However, it has an evident interaction with current density in affecting R_{ohmic}. In going from current densities of 0.33 A/cm^2 (15 A) to 0.44 A/cm^2 (20 A), there is a marked decrease in R_{ohmic} in the presence of 10% by volume of methanol vapor.

Moreover, it is interesting to notice the interactions between the effects of CO and CO_2. This interaction seems not to exist for R_{ohmic}. The same can be said for the rest of the frequency ranges at CO concentrations below 1% by volume. This however changes dramatically, in Fig. 5(b) and (c) R_{hf} and R_{if} increase significantly with increase in CO_2 as the CO concentration is raised to 2%.

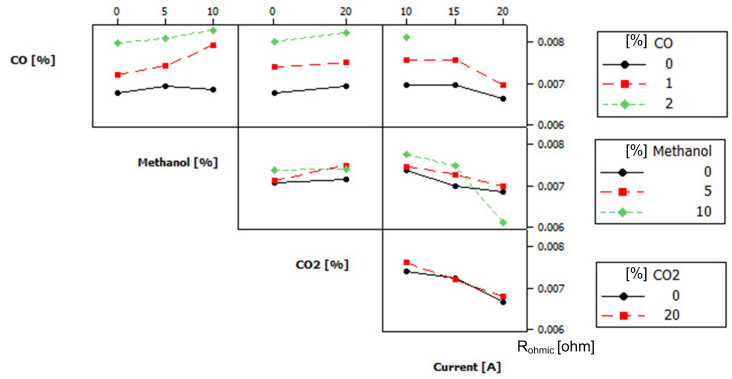

(a)

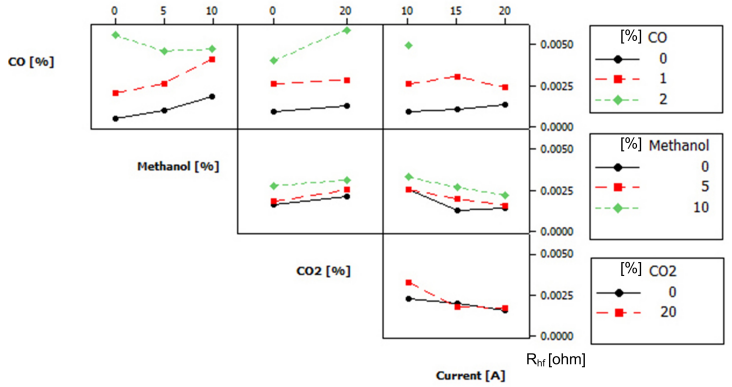

(b)

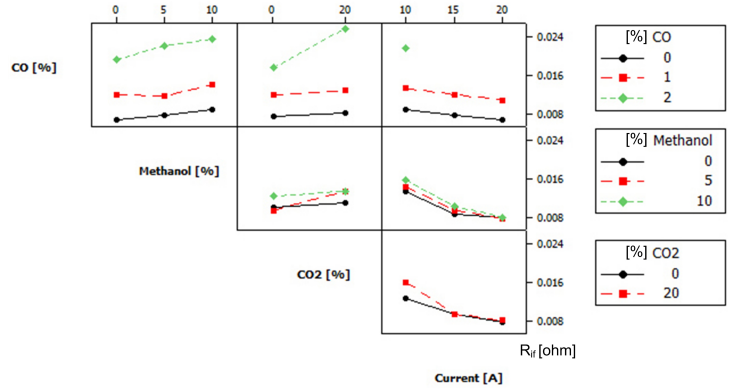

(c)

Figure 5: Interaction of effects among the different factors at 160°C (a) for ohmic resistance (b) high frequency resistance (c) intermediate - low frequency resistance

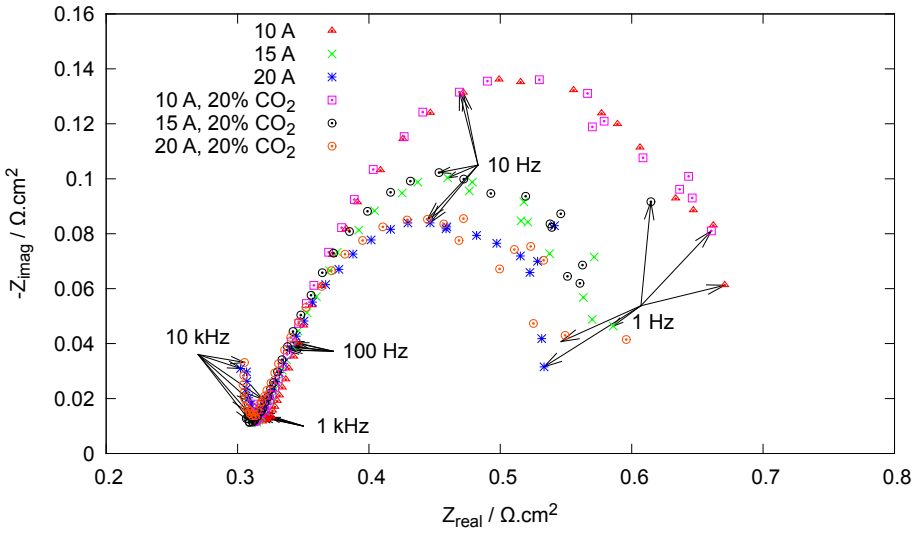

Figure 6: The effect of current density on a PBI-based HT-PEMFC operating at 160 °C both in the absence and in the presence of CO_2

3.2. Progressive EIS Analysis

3.2.1. Current Density

As already noted in other studies current density has the effect of increasing the activity in a cell [25, 17]. In Fig. 6 it can be seen that as current density increases from 0.22 A/cm^2 (10 A) to 0.33 A/cm^2 (15 A)and then 0.44 A/cm^2 (20 A), the total impedance decreases and both the real and imaginary components of the impedance drop causing the semi-circles to shrink.

Figure 6 shows also that the effects of current remains almost the same both in the case of pure H_2 gas and when 20% of the anode feed is CO_2. The only exception is seen at 10 A, where the high frequency semi-circle is slightly shifted to the left in the presence of 20% CO_2, while the low frequency one remains unaltered. This shows that CO_2 does not have significant effect on the losses of a fuel cell, especially in this case where the stoichiometric ratios are relatively high.

3.2.2. Methanol and CO_2

From the statistical analysis of main effects based on mean values of fitted resistances, it is seen that increase in the concentration of methanol causes increase in resistance in all frequency ranges. If we look closely into the fitted

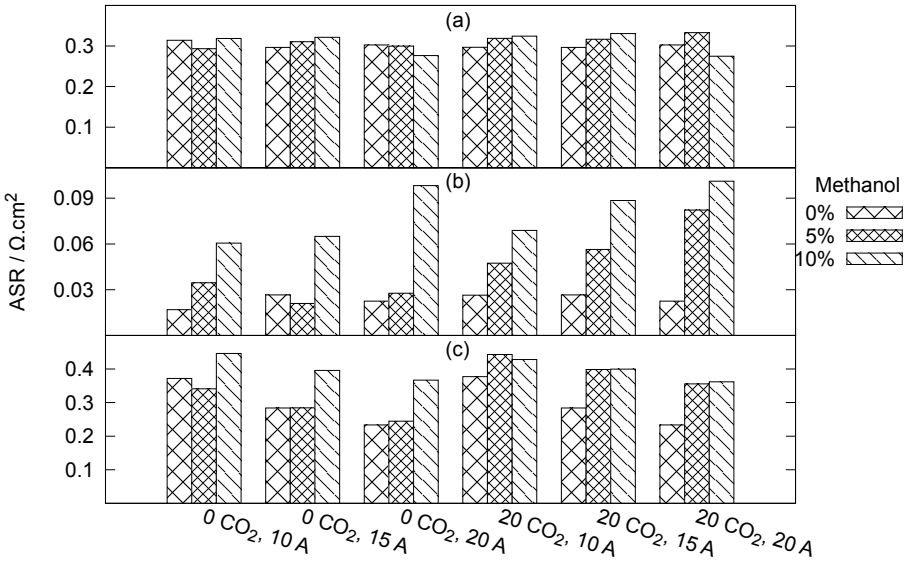

Figure 7: The effect of methanol on a PBI-based HT-PEMFC operating at 160 °C with changing CO_2 content and current density (a) ohmic resistance (b) high frequency resistance (c) intermediate - low frequency resistance

results we can see the different trends for different operating conditions and obtain some insight on the electrochemistry behind the effects.

The fits as displayed in Fig. 7 show the effect of methanol at 160 °C, where in Fig. 7(a) methanol seems to increase the R_{ohmic} for most of the operating conditions, with an exception at the highest current density tested 0.44 A/cm^2 (20 A). There is a slight decrease in the beginning as methanol is introduced, this could be because of the water vapor contained in the vapor mixture, which is said to enhance the proton conduction of the PBI-based membranes [29]. This however is seen only in the chronologically earlier measurements in the presence of methanol, perhaps before a full steady state was achieved. Continued introduction of methanol results in increased resistances instead of enhancing the proton conductivity of the membrane.

It is curious however, that the trend of R_{ohmic} changes whenever current density is raised to 0.44 A/cm^2. It is not clear whether this is a limitation of the electronic load used or the fuel cell itself. Such unstable behaviour was often recorded when the cell operated at the mentioned current density, especially when more impurities are present at the same time.

High frequency resistance in Fig. 7(b) is where the poisoning effects of

methanol are most clearly visible. Here, resistances increase with increase in methanol vapor concentration for all operating conditions almost linearly.

Intermediate-low frequency resistance in Fig. 7(c) also has similar trend as that of R_{hf} with increase in methanol content. It is interesting however, to notice that 5% methanol in the anode feed gas seems to have no effect in the absence of CO_2. This changes when CO_2 and methanol vapor are both present in the feed gas, where there is an evident increase in R_{if} for 5% methanol, but the effect of further increase in methanol content to 10 % is negligible. The same phenomenon is also seen to a smaller extent for R_{hf} in Fig. 7(b). Bottom line is that unlike in the case of pure hydrogen the effect of CO_2 is not negligible when methanol-water vapor mixture is present in the feed gas.

3.2.3. Methanol, CO_2 *and* CO

As it is already mentioned the effects of CO are the most severe to PEM fuel cells. It can be seen in Fig. 8 that the trends are similar to those without CO, where there is a general increase in resistances with increase in methanol content. A closer look at the data however reveals that the addition of CO causes all resistances to increase at all frequency sweeps with respect to the former case, where only Methanol and CO_2 were present. The increase is on average 8.6% for R_{ohmic}, 69% for R_{hf} and 61% for R_{if}.

The increase has small but fairly clear trend for R_{ohmic} and somewhat unclear trend for R_{if} as can be seen in Fig. 8(a) and Fig. 8(c), respectively. As in the case without CO the increase is most clearly visible for R_{hf}, Fig. 8(b). This similar trend of the resistances with increase in methanol content of the anode feed gas suggests that its effects do not depend on the presence CO. However, the effect of both impurities, methanol and CO, are dependent on CO_2 content. This means, since CO_2 content was varied equally in both cases, they each contribute to the sum of effects irrespective of the presence of the other.

As already observed in the interaction plots, the increase in resistances due to the addition of 1% by volume of CO in the anode feed are slightly more for operations in the presence of CO_2.

When CO content was raised to 2% the performance drop was exacerbated, and therefore only runs at 0.22 A/cm^2 (10 A) could be performed. While the trends remained similar in general, methanol had no effect on R_{hf} in the absence of CO_2.

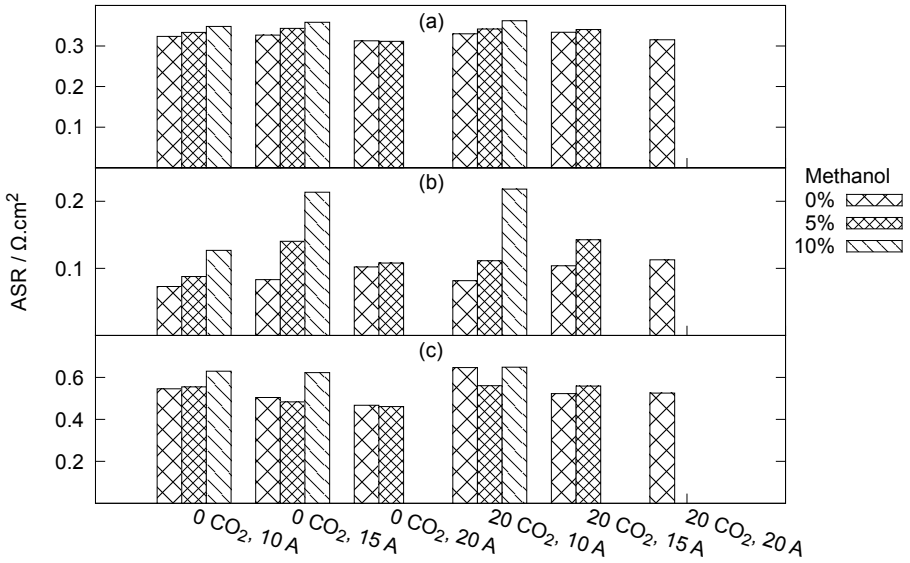

Figure 8: The effect of methanol on a PBI-based HT-PEMFC operating at 160 °C and in the presence of 1% by volume of CO with changing CO_2 content and current density (a) ohmic resistance (b) high frequency resistance (c) intermediate - low frequency resistance

4. Discussion

The purpose of this study was to characterize through experiments, the effects of all the impurities in reformate gas on a PBI-based HT-PEM fuel cell. This was done by means of impedance spectroscopy and it was found that all the impurities cause drop in cell performance at all the frequency sweeps performed.

Methanol, which is normally excluded from characterization tests, seems to have a poisoning effect at all frequency sweep ranges. The effects are interdependent with the effects of the other factors, especially with that of CO_2. The reason for fact that the interaction disappears in the case of 10% methanol could be because the effect of CO_2 is overwhelmed by that of methanol at such high concentrations.

It was observed that increase in methanol content increases almost all resistances. There is not much in the literature about the effects of methanol on HT-PEMFCs. It is reported that it is permeable, mainly via diffusion through H_3PO_4-doped PBI membrane [29, 30], and that it electro-oxidises on the surface of Pt electrodes [31, 32]. Moreover, methanol is known to undergo dehydrogenation on Pt surface according to the reaction below [32]:

$$CH_3OH + Pt \longrightarrow Pt{-}CO + 4\,H^+ + 4\,e^-$$

The fact that the poisoning effects are most clearly visible and proportional to the amount in feed gas at higher frequency ranges may suggest that it undergoes some reactions or adsorbs on the anode side, where high frequency activities dominate. One of these reactions could be the dehydrogenation reaction mentioned above that gives rise to intermediate CO formation, which may adsorb on the Pt surface and reduce the electroactive catalyst area. The performance drop could also be due to methanol crossover with subsequent electro-oxidation on the surface of platinum, as in the case of DMFCs [14].

The effects of current density, CO and CO_2 concentrations on the other hand are fairly well studied. The results obtained in this study show that increase in current density shrinks the impedance spectra causing the fitted resistances to decrease. Little or no effects were observed on R_{ohmic} and R_{hf} with change in current density. Similar negligible effect on R_{hf} is also seen in [33]. Concerning R_{ohmic} however, according to [17] there is increase in water production with increase in current density which may enhance the conductivity of the PBI-based membrane. This would imply a decrease in R_{ohmic}, which is not seen in this study, except for a very slight decrease in going from 0.22 A/cm^2 to 0.33 A/cm^2.

Most of the effects of current density are displayed on R_{if}. This may be attributed to the increase in the flow of gases, as the hydrogen demand is calculated based on Faraday's law, in which more current corresponds to more hydrogen, and consequently air.

The results of this study show that tolerance to CO depends on the concentrations of the other constituents of the reformate gas, namely CO_2 and unconverted methanol-water vapor mixture. In the presence of 20% by volume of CO_2 and 5% methanol, putting more than 1% CO has a very detrimental effect on the fuel cell, especially at higher current densities. This increase in the poisoning effects of CO in the presence of CO_2 is also seen in the interaction plots, where the most important interaction is seen for CO and CO_2 at CO concentration of 2% by volume. This suggests that tolerance to CO of a PBI-based HT-PEMFC may be compromised by the presence of CO_2 in the anode feed. This interaction is also seen in [26] for R_{hf}.

The fact that the poisoning effects of CO are most important for R_{hf} and R_{if} confirms the notion that CO affects mainly Pt electro-catalyst [9]. It adsorbs on the active Pt sites of the electrodes, both anode and cathode

(maybe through CO crossover) and inhibits the respective half-cell reactions, without affecting so much the proton conductivity of the electrolyte. The effect of CO poisoning on both anode and cathode is also reported in [13].

The interaction among effects obtained in this study is a valuable information, as it gives an idea of best tolerable mixes of impurities for optimizing the operating parameters of an HT-PEMFC. This can be an input for tweaking the performance and selectivity of both the fuel cell and the methanol reforming processor.

5. Conclusions

In an experimental characterization of a PBI-based HT-PEMFC, the effects of impurities from methanol steam reforming were investigated by means of EIS. It was found that all the impurities in the reformate gas have poisoning effects on the cell. This is true whether they are introduced individually or collectively as a stream of gases and vapors. The most severe effects are observed in the presence of CO, while CO_2 on the other hand has a very minor effects if present alone.

Statistical analysis showed some of the possible interdependence among the effects of the different impurities. The interaction is most important for CO and CO_2 at CO concentration of 2% by volume, suggesting that tolerance to CO of a PBI-based HT-PEMFC may be compromised by the presence of CO_2 in the anode feed gas. Current density was also varied, where the performance drop exacerbated at above 0.33 A/cm^2 and high concentration of impurities.

The presence of methanol was found to increase the resistance at all the frequency ranges and therefore it should be considered when optimizing the operating parameters of a reformate gas-fed HT-PEMFC. The increase is small, comparable to that of CO_2, at 5% by volume for R_{ohmic}, but more important at 10% by volume for R_{hf}. Its interactions are mainly with CO_2, especially at 5% by volume of vapor mixture. This calls for more consideration of methanol during characterization studies of the poisoning of an HT-PEMFC operating on a reformate gas, mainly because tolerance to CO is reduced in the presence of other impurities.

To have an even more complete picture of all factors, the effect of time should be considered and interdependence with the other factors investigated. Future works should also include the modeling of adsorption/desorption of CO and methanol, and experimental investigation of methanol crossover and

its electro-oxidation on Pt electro-catalyst. This could explain many of the poisoning effects that are explored in the present work, and bring to light whether the poisoning effect is by means of crossover with subsequent electro-oxidation on the cathode as in the case of DMFC or other phenomena are involved.

Appendix A

Table .2: Appendix A: Full multilevel factorial design of experiment with resistance responses

Run	y_{CO} [%]	y_{CH_3OH} [%]	y_{CO_2} [%]	i $[A/cm^2]$	R_{ohmic} [Ω]	R_{hf} [Ω]	R_{if} [Ω]
1	0	0	0	10	0.006978	0.000375	0.008262
2	0	0	0	15	0.006588	0.000591	0.00631
3	0	0	0	20	0.006723	0.000501	0.005188
4	0	0	20	10	0.006786	0.000441	0.008352
5	0	0	20	15	0.006733	0.000418	0.006265
6	0	0	20	20	0.006761	0.000461	0.005353
7	0	5	0	10	0.006522	0.000768	0.007576
8	0	5	0	15	0.006901	0.000467	0.006321
9	0	5	0	20	0.00666	0.000616	0.005433
10	0	5	20	10	0.00709	0.001053	0.009849
11	0	5	20	15	0.007036	0.001254	0.008853
12	0	5	20	20	0.007396	0.001828	0.007906
13	0	10	0	10	0.007081	0.001347	0.009917
14	0	10	0	15	0.007145	0.001443	0.008795
15	0	10	0	20	0.006143	0.002184	0.008151
16	0	10	20	10	0.007205	0.001531	0.009516
17	0	10	20	15	0.007346	0.001967	0.008883
18	0	10	20	20	0.006109	0.002248	0.00804
19	1	0	0	10	0.007195	0.001621	0.012131
20	1	0	0	15	0.007266	0.00185	0.011213
21	1	0	0	20	0.006953	0.002268	0.010385
22	1	0	20	10	0.007332	0.001815	0.014375
23	1	0	20	15	0.007422	0.002308	0.011624
24	1	0	20	20	0.007012	0.002505	0.011667
25	1	5	0	10	0.007415	0.001953	0.012338
26	1	5	0	15	0.007631	0.003117	0.010746
27	1	5	0	20	0.006924	0.002399	0.010242
28	1	5	20	10	0.007595	0.002473	0.012453
29	1	5	20	15	0.007568	0.003169	0.012412
30	1	5	20	20	*	*	*

Continued on next page

Table .2 – continued from previous page

Run	y_{CO} [%]	y_{CH_3OH} [%]	y_{CO_2} [%]	i [A/cm^2]	R_{ohmic} [Ω]	R_{hf} [Ω]	R_{if} [Ω]
31	1	10	0	10	0.007742	0.002819	0.013995
32	1	10	0	15	0.007966	0.004745	0.013847
33	1	10	0	20	*	*	*
34	1	10	20	10	0.008049	0.004848	0.014416
35	1	10	20	15	*	*	*
36	1	10	20	20	*	*	*
37	2	0	0	10	0.00788	0.004276	0.018095
38	2	0	0	15	*	*	*
39	2	0	0	20	*	*	*
40	2	0	20	10	0.008071	0.006932	0.020383
41	2	0	20	15	*	*	*
42	2	0	20	20	*	*	*
43	2	5	0	10	0.007888	0.003611	0.014432
44	2	5	0	15	*	*	*
45	2	5	0	20	*	*	*
46	2	5	20	10	0.008313	0.005642	0.029976
47	2	5	20	15	*	*	*
48	2	5	20	20	*	*	*
49	2	10	0	10	0.008251	0.004265	0.020079
50	2	10	0	15	*	*	*
51	2	10	0	20	*	*	*
52	2	10	20	10	0.008337	0.005189	0.027023
53	2	10	20	15	*	*	*
54	2	10	20	20	*	*	*

References

[1] Bromberg L and Cheng W K. Methanol as an Alternative Transportation Fuel in the U.S.: Options for Sustainable and/or Energy-Secure Transportation. Technical report, Massachusetts Institute of Technology, Sloan Laboratories for Automotive and Aircraft Engines Cambridge, MA 02139 USA Battelle Columbus, OH USA, 2010-11.

[2] George A. Olah, Alain Goeppert, and G. K. Surya Prakash. *Beyond Oil and Gas: The Methanol Economy*. Wiley, September 2009.

[3] Methanex Corporation®. Technical Information and Safe Handling Guide for Methanol. 2006.

[4] Chao Pan, Ronghuan He, Qingfeng Li, Jens Oluf Jensen, Niels J. Bjerrum, Henrik Andersen Hjulmand, and Anders Brsting Jensen. Integration of high temperature PEM fuel cells with a methanol reformer. *Journal of Power Sources*, 145(2):392 – 398, 2005. Selected papers presented at the Fuel Cells Science and Technology Meeting.

[5] Martha Ouzounidou, Dimitris Ipsakis, Spyros Voutetakis, Simira Papadopoulou, and Panos Seferlis. A combined methanol autothermal steam reforming and PEM fuel cell pilot plant unit: Experimental and simulation studies. *Energy*, 34(10):1733 – 1743, 2009. 11th Conference on Process Integration, Modelling and Optimisation for Energy Saving and Pollution Reduction.

[6] Krishan kumar Bhatia. *Study of Methanol Reforming Polymer Electrolyte Fuel Cell System*. PhD thesis, The Pennsylvania State University, The Graduate School, College of Engineering, August 2004.

[7] Søren Juhl Andreasen, Jakob Rabjerg Vang, and Søren Knudsen Kær. High temperature PEM fuel cell performance characterisation with CO and CO_2 using electrochemical impedance spectroscopy. *International Journal of Hydrogen Energy*, 36(16):9815 – 9830, 2011. European Fuel Cell 2009.

[8] Felix N. Bchi, Minoru Inaba, and Thomas J. Schmidt. *Polymer Electrolyte Fuel Cell Durability*. Springer New York, 2009.

[9] Jianlu Zhang, Zhong Xie, Jiujun Zhang, Yanghua Tang, Chaojie Song, Titichai Navessin, Zhiqing Shi, Datong Song, Haijiang Wang, David P. Wilkinson, Zhong-Sheng Liu, and Steven Holdcroft. High temperature PEM fuel cells. volume 160, pages 872 – 891. 2006. Special issue including selected papers presented at the International Workshop on Molten Carbonate Fuel Cells and Related Science and Technology 2005 together with regular papers.

[10] Susanta K. Das, Antonio Reis, and K.J. Berry. Experimental evaluation of CO poisoning on the performance of a high temperature proton exchange membrane fuel cell. *Journal of Power Sources*, 193(2):691 – 698, 2009.

[11] Wei-Mon Yan, Hsin-Sen Chu, Meng-Xi Lu, Fang-Bor Weng, Guo-Bin Jung, and Chi-Yuan Lee. Degradation of proton exchange membrane fuel cells due to CO and CO2 poisoning. *Journal of Power Sources*, 188(1):141 – 147, 2009.

[12] Marucchi-Soos E.P. Buckley D.T. Bellows, R.J. Analysis of Reaction Kinetics for Carbon Monoxide and Carbon Dioxide on Polycrystalline Platinum Relative to Fuel Cell Operation. *Industrial and Engineering Chemistry Research*, 35(4):1235–1242, 1996. cited By (since 1996) 67.

[13] Xuan Cheng, Zheng Shi, Nancy Glass, Lu Zhang, Jiujun Zhang, Datong Song, Zhong-Sheng Liu, Haijiang Wang, and Jun Shen. A review of PEM hydrogen fuel cell contamination: Impacts, mechanisms, and mitigation. *Journal of Power Sources*, 165(2):739 – 756, 2007. IBA HBC 2006, Selected papers from the INTERNATIONAL BATTERY ASSOCIATION & HAWAII BATTERY CONFERENCE 2006 Waikoloa, Hawaii, USA 9-12 January 2006.

[14] C.Y. Du, T.S. Zhao, and W.W. Yang. Effect of methanol crossover on the cathode behavior of a DMFC: A half-cell investigation. *Electrochimica Acta*, 52(16):5266 – 5271, 2007.

[15] Samuel S. Araya, Søren K. Kær, and Søren J. Andreasen. Vapor Delivery Systems for the Study of the Effects of Reformate Gas Impurities in HT-PEM Fuel Cells. *Journal of Fuel Cell Science and Technology*, 9(1):015001, 2012.

[16] Xiao-Zi Yuan, Chaojie Song, Haijiang Wang, and Jiujun Zhang. *Electrochemical Impedance Spectroscopy in PEM Fuel Cells: Fundamentals and Applications*. Springer, 2010.

[17] M. Mamlouk and K. Scott. Analysis of high temperature polymer electrolyte membrane fuel cell electrodes using electrochemical impedance spectroscopy. *Electrochimica Acta*, 56(16):5493 – 5512, 2011.

[18] Jianlu Zhang, Lei Zhang, Cicero W.B. Bezerra, Hui Li, Zetao Xia, Jiujun Zhang, Aldala L.B. Marques, and Edmar P. Marques. EIS-assisted performance analysis of non-noble metal electrocatalyst (FeN/C)-based PEM fuel cells in the temperature range of 23-80 °C. *Electrochimica Acta*, 54(6):1737 – 1743, 2009.

[19] Saeed Asghari, Ali Mokmeli, and Mahrokh Samavati. Study of PEM fuel cell performance by electrochemical impedance spectroscopy. *International Journal of Hydrogen Energy*, 35(17):9283 – 9290, 2010. The 1st Iranian Conference On Hydrogen & Fuel Cell.

[20] N. Fouquet, C. Doulet, C. Nouillant, G. Dauphin-Tanguy, and B. Ould-Bouamama. Model based PEM fuel cell state-of-health monitoring via ac impedance measurements. *Journal of Power Sources*, 159(2):905 – 913, 2006.

[21] Kengkaj Pattamarat and Mali Hunsom. Testing of PEM fuel cell performance by electrochemical impedance spectroscopy: Optimum condition for low relative humidification cathode. *Korean Journal of Chemical Engineering*, 25:245–252, 2008. 10.1007/s11814-008-0044-z.

[22] Evgenij Barsoukov and J. Ross Macdonald. *Impedance Spectroscopy: Theory, Experiment, and Applications*. Wiley - Interscience, 2nd edition edition, April 2005.

[23] Mark E. Orazem and Bernard Tribollet. *Electrochemical Impedance Spectroscopy*. John Wiley & Sons, Inc., 2008.

[24] Paul Monk. *Fundamentals of Electroanalytical Chemistry*. Analytical Techniques in the Sciences. John Wiley & Sons, Ltd., 20 MAR 2007.

[25] Xiaozi Yuan, Haijiang Wang, Jian Colin Sun, and Jiujun Zhang. AC impedance technique in PEM fuel cell diagnosis–A review. *International Journal of Hydrogen Energy*, 32(17):4365 – 4380, 2007. Fuel Cells.

[26] Søren Juhl Andreasen, Rasmus Mosbæk, Jakob Rabjerg Vang, Søren Knudsen Kær, and Samuel Simon Araya. EIS Characterization of the Poisoning Effects of CO and CO_2 on a PBI Based HT-PEM Fuel Cell. *ASME Conference Proceedings*, 2010(44045):27–36, 2010.

[27] Ryan P. O'Hayre, Suk-Won Cha, Whitney G. Colella, and Fritz B. Prinz. *Fuel Cell Fundamentals*. John Wiley & Sons, Inc., 2008.

[28] Y.-T. Tsai and D.H. Whitmore. Nonlinear least-squares analyses of complex impedance and admittance data for solid electrolytes. *Solid State Ionics*, 7(2):129 – 139, 1982.

[29] Maria K. Daletou, Joannis K. Kallitsis, George Voyiatzis, and Stylianos G. Neophytides. The Interaction of Water Vapors with H_3PO_4 Imbibed Electrolyte Based on PBI/polysulfone Copolymer Blends. *Journal of Membrane Science*, 326(1):76 – 83, 2009.

[30] Qingfeng Li, Jens Oluf Jensen, Robert F. Savinell, and Niels J. Bjerrum. High Temperature Proton Exchange Membranes Based on Polybenzimidazoles for Fuel Cells. *Progress in Polymer Science*, 34(5):449 – 477, 2009.

[31] S Sriramulu, T.D Jarvi, and E.M Stuve. Reaction mechanism and dynamics of methanol electrooxidation on platinum(111). *Journal of Electroanalytical Chemistry*, 467(1-2):132 – 142, 1999.

[32] J.S. Spendelow, P.K. Babu, and A. Wieckowski. Electrocatalytic oxidation of carbon monoxide and methanol on platinum surfaces decorated with ruthenium. *Current Opinion in Solid State and Materials Science*, 9(12):37 – 48, 2005.

[33] Rohit Makharia, Mark F. Mathias, and Daniel R. Baker. Measurement of Catalyst Layer Electrolyte Resistance in PEFCs Using Electrochemical Impedance Spectroscopy. *Journal of The Electrochemical Society*, 152(5):A970–A977, 2005.